

Theoretical Study on the Thermoelectric Properties of Porous Armchair Graphene Nanoribbons

Navjotkaur¹, Deep Kamal Kaur Randhawa² and Sukhdeep Kaur^{3*}

^{1&3}Department of Electronics Technology, Guru Nanak Dev University, Amritsar, Punjab, India

²Department of Electronics and Communication Engineering, Guru Nanak Dev University, RC Jalandhar, Punjab, India

*Corresponding Author

E-Mail: navjotriar@gmail.com, randhawadk@gmail.com, gndusukhdeep@gmail.com

(Received 12 April 2019; Revised 30 April 2019; Accepted 20 May 2019; Available online 27 May 2019)

Abstract - Thermoelectric properties of porous graphene nanoribbons (GNRs) have been explored for a range of pore dimensions in order to achieve a high performance one-dimensional nanoscale thermoelectric device. In this paper, study has been done to observe the effect of different nanoporous shapes and their associated positions on the thermoelectric properties of GNRs. The aim of this work is to study the effect of various circular, triangular, rectangular and rhombus shape dimensions so as to tune the pore to its optimal dimension that would enhance the overall thermoelectric efficiency. Further, the effect of passivation of pore edges has been studied for all shapes so as to observe its effect on thermoelectric performance. Also, the effect of temperature dependence on thermoelectric efficiency has been studied. Ballistic transport regime and semi empirical method using Huckel basis set is used to obtain the electrical properties while the tersoff potential is used for the phononic system.

Keywords: Thermoelectric, Nanopore, Figure of Merit, Passivation

I. INTRODUCTION

Graphene is a two-dimensional (2D) allotrope of carbon which has attracted much attention due to its superior electrical, mechanical and thermal properties. One potentially promising application for graphene could be in the field of thermo electronics[1]. In the mid-1990s, the achievement in the improvement of thermoelectric performance in nanostructured materials due to phonon boundary scattering and lateral quantum confinement of electrons[2] was theoretically predicted. The thermal conductivity can be reduced by nanostructuring them into nanoribbons. This decrease could be further engineered in porous nanoribbons, since phonon thermal conductivity is reduced in nanoporous semiconductors[3]. The efficiency of a thermoelectric device and material is determined by its thermoelectric figure of merit (ZT) defined as: $ZT = S^2GT/\kappa$ where S is the Seebeck coefficient (thermopower), G is the electrical conductance, T the temperature and $\kappa = \kappa_e + \kappa_{ph}$ the thermal conductance given by κ , where κ_e (κ_{ph}) is the electronic (phononic) contribution to κ . Clearly ZT could be enhanced by increasing the power factor (S^2GT) or decreasing the thermal conductance and therefore a high-performance thermoelectric material should possess a large Seebeck coefficient and electrical conductance and simultaneously a low thermal conductance. The search for new materials with enhanced thermal properties continues to intensify, because these factors are correlated and

increasing ZT to values greater than unity requires a delicate optimization of several material properties[4].

Several theoretical studies have been carried out to investigate the performance of graphene and graphene nanoribbons (GNRs). Hossain *et al.*, [5] have introduced rectangular nanopores in the nanoribbon and tuned the pore to its optimal dimension which results in superior ZT which is six times higher than pristine GNRs. According to the study done by Yijian Ouyang *et al.* [6] the magnitude of the thermopower increases as the GNR becomes more defective. Although both the increase in the thermopower and the decrease in the thermal conductance can increase the ZT factor, the degradation of the electronic conductance outweighs them and with the increased number of defects the ZT factor decreases.

Yong Xu *et al.*, [7] have shown in their work that the superior thermal conductivity of graphene is contributed not only by large ballistic thermal conductance but also by very long phonon mean free path (MFP). The long phonon MFP is explained by the low dimensional nature and high sample purity of graphene. It results in important isotope effects and size effects on thermal conduction. Introduction of rough boundaries and weakly-coupled interfaces are promising ways to suppress thermal conduction effectively. Chang-Ning Pan, *et al.*, [8] have studied ballistic thermoelectric properties in graphene-nanoribbon-based heterojunctions by using the non-equilibrium Green's function approach and the Landauer transport theory. Their results show that for the different heterojunctions, the phonon thermal conductance has similar effects. Along with this high sensitivity of the electron transport is seen along with the geometry details of the heterojunctions. The thermopower can be strongly enhanced by the fluctuations of electronic transmissions. With optimization of the thermopower, together with suppression of phonon transport by mismatching interface structures, the high thermoelectric figure of merit $ZT \sim 0.6$ at room temperature $T=300K$ and $ZT \sim 0.9$ at low temperature $T=100K$ is obtained.

Also Liang *et al.*, [9] studied graphene nano wiggles GNWs employing resonant tunneling effect and found the enhanced values of ZT. Their devices were predicted to achieve a ZT of 0.79 at room temperature. By introducing edge roughness in zigzag GNRS, Sevincli *et al.*, [10] have predicted that a

ZT of 4 can be achieved. Although there is no experimental validation of the above work as it is only theoretical, there are some groups who have experimentally investigated the thermopower of graphene[5,11-13]

The proposed device is an armchair graphene nanoribbon based structure. Thermal conductivity is less in case of armchair GNRs when compared with ZGNRs of same dimensions[5]. Also they show pore dimension dependent transport parameters accounting for their selection. Graphene has been the center stage of research recently. Its synthesis techniques[14-16] such as electron beam lithography,[17] the use of nanowires as etch mask[18] and molecular templating have greatly advanced, allowing precise fabrication of GNRs[5]. However, drilling pores in GNRs with atomistic precision is a challenging task. Nevertheless, techniques like transmission electron microscopy[19,20] and helium ion beam milling[21-23] can also be used to drill pores in GNRs with precise control. This supports the realization of the device proposed in this paper.

II. METHODOLOGY

In this paper, we propose a new thermoelectric device structure based on armchair GNRs embedded with the circular, triangular, rectangular and rhombus pores at various positions. Also the effect of pore passivation is observed. By varying the shape and position of the pore we can superior electrical conductivity as the introduction of the pore reduces thermal conductivity. These two factors lead to enhanced thermoelectric performance. The thermoelectric performance of a material is measured in terms of dimensionless figure of merit:

$$ZT = \frac{S^2 G T}{\kappa_e + \kappa_{ph}}$$

Within the Extended Huckel theory framework, $G^R = (ES_{ov} - H - \Sigma_L - \Sigma_R)^{-1}$ is the retarded Green function where E is the electron energy, H and S_{ov} are the Hamiltonian and overlap matrix of the central region respectively which are calculated from extended Huckel technique using Hoffman basis[23]. Once the retarded Green's function is obtained, the electron transmission function can be obtained through:

$$T(E) = \text{Trace}[\Gamma_R(E) G^R(E) \Gamma_L(E) G^{R\dagger}(E)] \quad (1)$$

where $\Gamma_{L,R}(E) = i(\Sigma_{L,R}(E) - \Sigma_{L,R\dagger}(E))$ describes the level broadening due to the coupling between the left / right electrodes and the central scattering region and $\Sigma_{L,R}(E)$ are the retarded self-energies for the electrodes. The mesh points in real space calculation are $1 \times 1 \times 100$ k points, mesh cut-off at 10 Hartree and the temperature was set at 300K. Once $T(E)$ is known, Seebeck Coefficient S , electrical conductance G and electronic thermal conductance k_e can be obtained under linear response approximation as[24]:

$$G = \frac{I}{\Delta V} \Big|_{\Delta T=0} = e^2 L_0 \quad (2)$$

$$S = \frac{\Delta V}{\Delta T} \Big|_{I=0} = \frac{L_1}{e T L_0} \quad (3)$$

$$k_e = \frac{I_Q}{\Delta T} \Big|_{I=0} = \frac{L_2 - L_1^2/L_0}{T} \quad (4)$$

Where

$$L_n = \frac{2}{h} \int dE T(E) \left(-\frac{\partial f}{\partial E}\right) (E - \mu)^n \quad (5)$$

Here L_n is Lorenz function, e is the charge of electron, h is the Planck constant, μ is the chemical potential, T is the average temperature and $\partial f / \partial E$ is the derivative[25] of the Fermi function ($f = 1 + \exp((E - \mu)/k_B T)^{-1}$) known as Fermi-Dirac distribution function. To calculate the phonon thermal conductance, we used the Landauer approach[26]:

$$k_{ph} = \frac{\hbar^2}{2\pi k_B T^2} \int d\omega \omega^2 T_{ph}(\omega) \left(\frac{\partial n}{\partial \omega}\right) \quad (6)$$

For phonon transmission $T_{ph}(\omega)$, H and S are substituted by a force constant matrix K , and a diagonal matrix of atomic mass M respectively. The term $\partial n / \partial \omega$ is the derivative of the Bose-Einstein distribution for phonons. To calculate the force constant matrix for phonons, empirical Tersoff potential (Tersoff_CH_2005) was used. Both the electron and phonon transport simulations are performed in the virtual nanolab-Atomistix toolkit (ATK) software package[27]. Each structure is optimized before transport calculations with its atom coordinates relaxed so that the forces on individual atoms are minimized to be smaller than 0.01 eV \AA^{-1} . Since the mean free path for electro-acoustic phonon scattering in graphene (greater than $2 \mu\text{m}$) is much larger than our proposed model, the electron-phonon interactions are neglected while carrying out independent electron and phonon calculations[28].

III. RESULTS AND DISCUSSION

The width W_r and length L_r of the ribbon has been kept constant at 2.46nm (21 atoms wide) and 8.1nm respectively, while the pore shape and its associated position has been varied to achieve superior performance[29]. Different pore positions corresponding to centre and respective edges (left and right) of the nanoribbon has been evaluated. Further, the effect of increasing the nanopores from single to double has been predicted. The symmetry of the pores is maintained in each case. In the later section, the change in thermoelectric performance due to temperature dependence is also studied.

A. Circular Pore

The atomistic model of our proposed armchair graphene ribbon structures with circular pores is shown in Fig.1. As it shows, each pore has its own associated edge terminations with two channels on both sides of the nanoribbon. The pore size is kept constant at a diameter of 1.23nm.

The variation in values of parameters S , G , K_{ph} and ZT are plotted with respect to chemical potential of the nanopore. As shown in Fig (2(d)) the peak of ZT is observed at -0.51 eV and its value is 0.329. To obtain better figure of merit the value of power factor ($S^2 G$) should be higher. From the Fig(2(a),(c)) it is seen that the decrease in G is compensated with higher value of S at that point. In addition, the thermal conductivity is reduced significantly

which in turn leads to the enhancement of figure of merit. The two pore circular structure shows the best result

among the other pores.

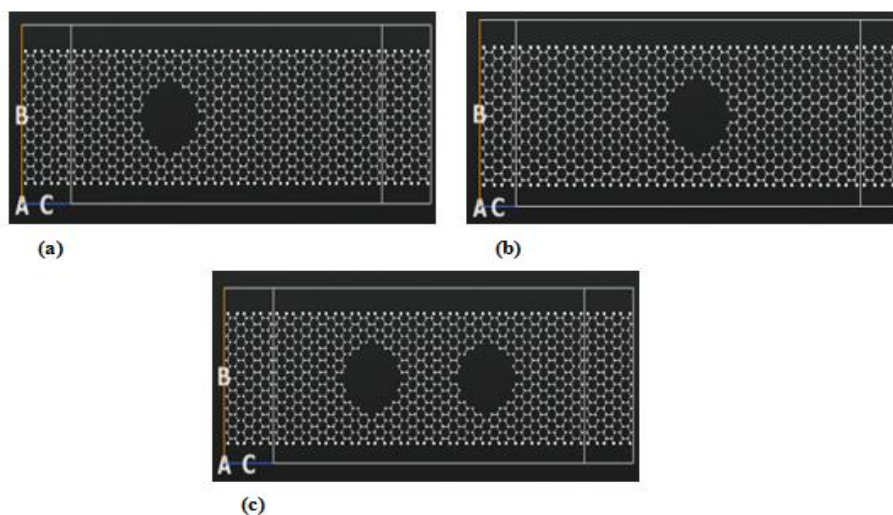


Fig. 1 Geometrical optimized structure of the graphene nanoribbon with circular nanopore thermoelectric device with pore diameter 1.23nm

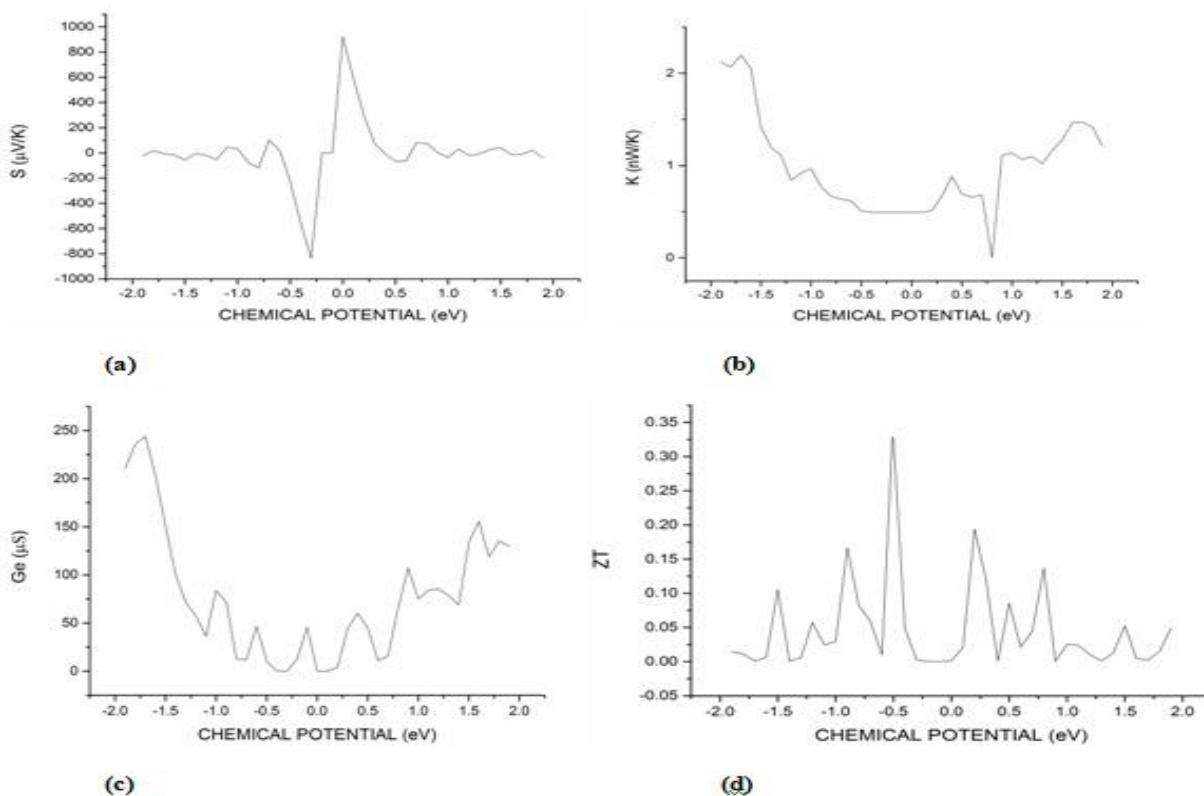


Fig.2 (a) Seebeck coefficient, (b) thermal conductivity, (c) conductance, and (d) figure of merit for the circular nanopore

B. Rectangular Pore

The atomistic model of our proposed armchair graphene ribbon structures with rectangular pores is shown in Fig (3). As it shows each pore has its own associated edge terminations with two channels on both sides of the nanoribbon. The length of the pore is 1.846nm and its width is 0.984nm. The variation in values of parameters S, G, Kph

and ZT are plotted with respect to chemical potential of the nanopore. The peak of ZT is observed at -0.72eV and its value is 0.4237. From the Fig(4(b)) it is seen that the value of thermal conductivity is consistently low. At the chemical potential where the ZT is maximum the decrease in G is compensated by increase in S. Hence this leads to the increase in the value of figure of merit. The two pore rectangular shape GNR shows the optimum result.

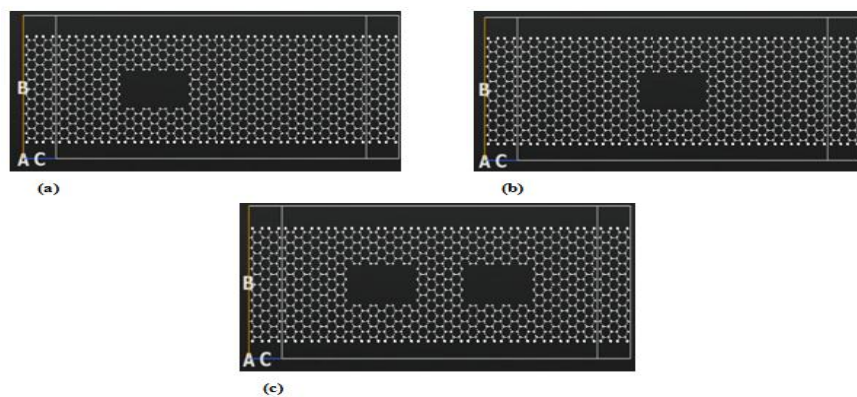


Fig. 3 Geometrical optimized structure of the graphene nanoribbon with rectangular nanopore thermoelectric device with pore length 1.846nm, width 0.984nm

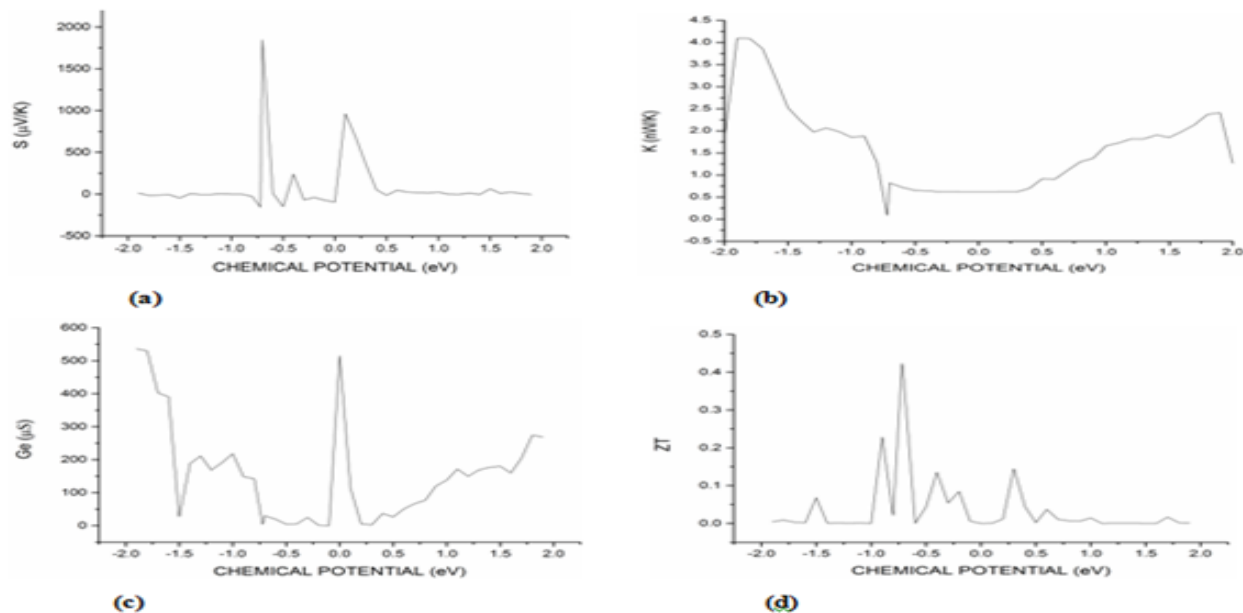


Fig. 4 (a) Seebeck coefficient, (b) thermal conductivity, (c) conductance, and (d) figure of merit for the rectangular nanopore

C. Triangular Pore

The atomistic model of our proposed armchair graphene ribbon structures with triangular pores is shown in Fig (5). As it shows each pore has its own associated edge terminations with two channels on both sides of the nanoribbon. The geometry of the triangular pore is equilateral in nature. The side of the pore is 2.272nm. The variation in values of parameters S, G, Kph and ZT are plotted with respect to chemical potential of the nanopore. The peak of ZT is observed at 0.10eV and its value is 0.2055. From the Fig (6(a), (c)) it is seen that the decrease in G is compensated by higher value of S at 0.10eV point. The thermal conductivity is reduced significantly which in turn leads to the enhancement of figure of merit. The two pore triangular structure shows the best result among the other pores.

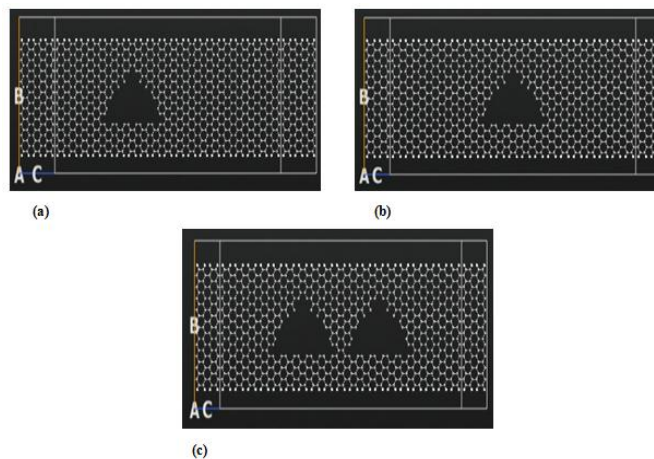


Fig. 5 Geometrical optimized structure of the graphene nanoribbon with triangular nanopore thermoelectric device with pore side 2.272nm and (d) passivated triangular two pore structure

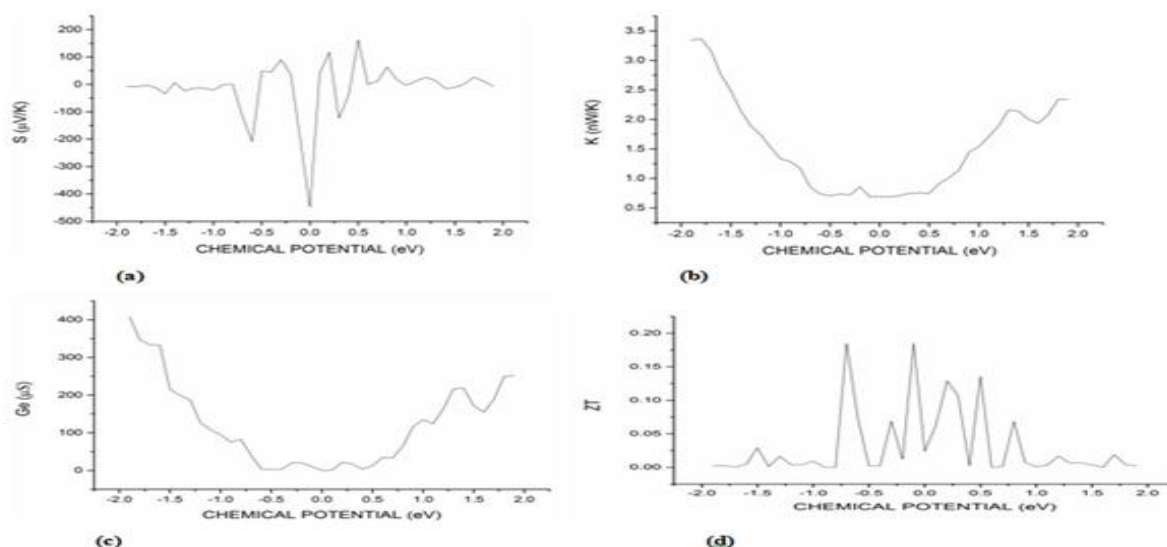


Fig. 6(a) Seebeck coefficient, (b) thermal conductivity, (c) conductance, and (d) figure of merit for the triangular nanopore

D. Rhombus Pore

The atomistic model of our proposed armchair graphene nanoribbon structure with rhombus pores is shown in Fig(7).As it shows each pore has its own associated edge terminations with two channels on both sides of the nanoribbon. The sides of the rhombus pore are equal in nature. The value of the side of rhombus is 1.353nm.The variation in values of parameters S, G, Kph and ZT are plotted with respect to chemical potential of the nanopore. As shown in Fig (8) the peak of ZT is observed at -0.72eV and its value is 0.3328. From the Fig (8(a),(c)) it is seen that the decrease in S is compensated by higher value of G. The thermal conductivity is reduced significantly which in turn leads to the enhancement of figure of merit. The two pore rhombus structure shows the best result among the other pores.

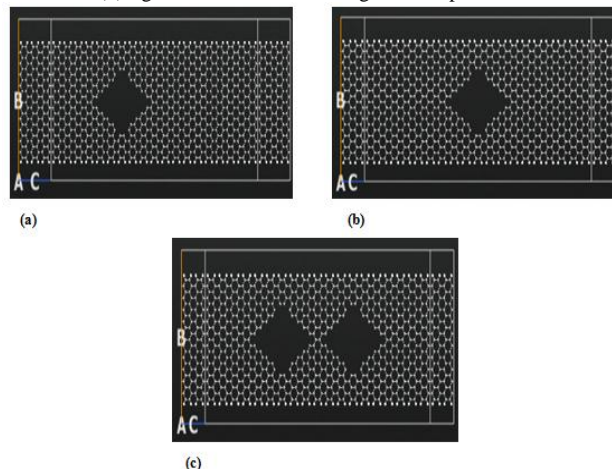


Fig. 7 Geometrical optimized structure of the graphene nanoribbon with rhombus nanopore thermoelectric device with pore side 1.353nm

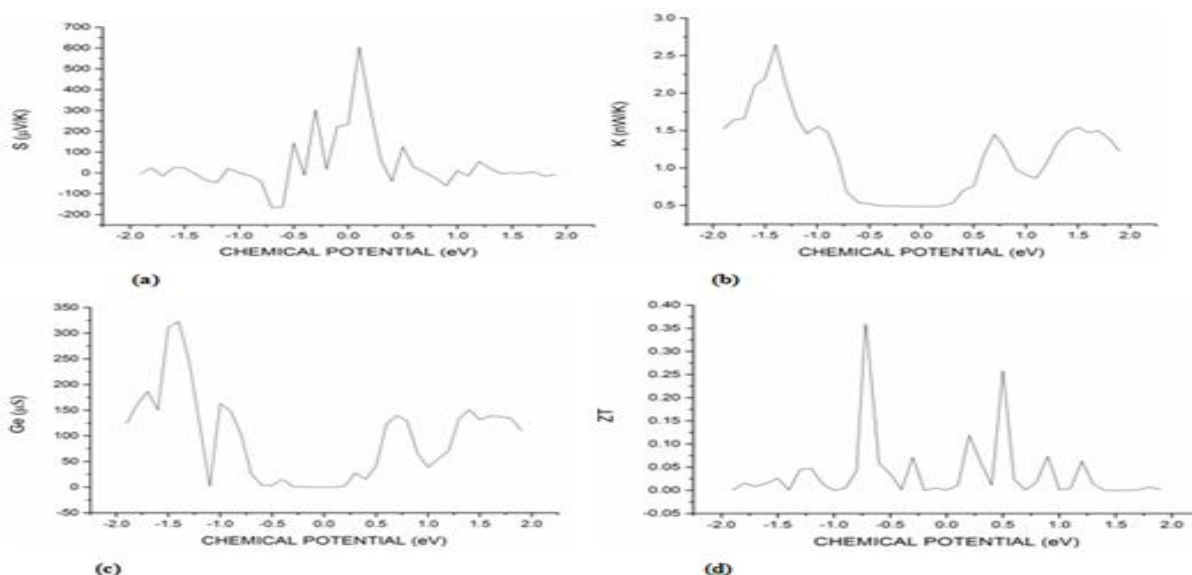


Fig. 8 (a) Seebeck coefficient, (b) thermal conductivity, (c) conductance, and (d) figure of merit for the rhombus nanopore

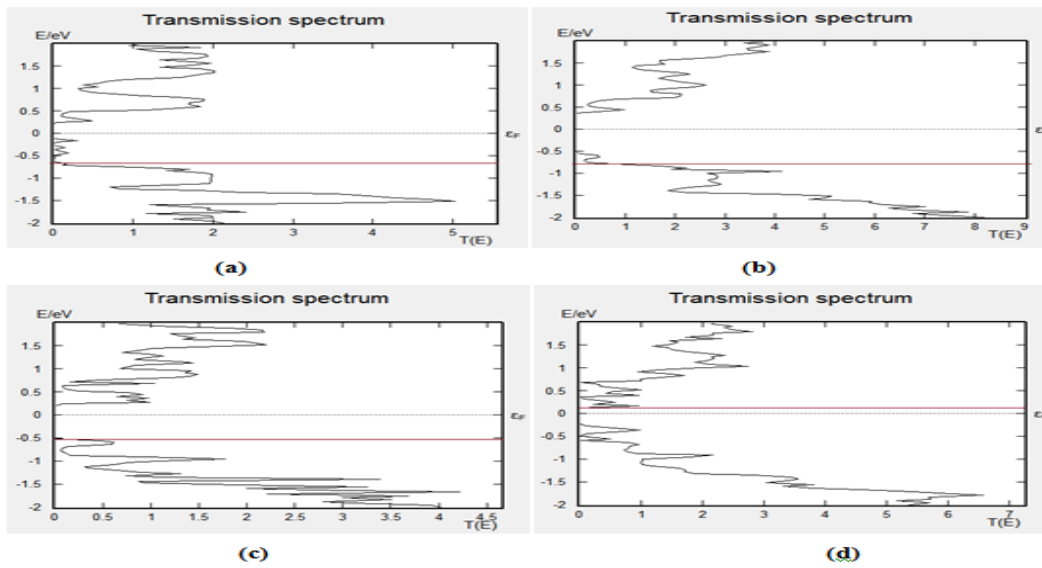


Fig. 9 Transmission spectrum of (a) Circular pore, (b) Rectangular pore, (c) Rhombus pore and (d) Triangular pore GNR

IV. COMPARISON OF ALL THE PORES

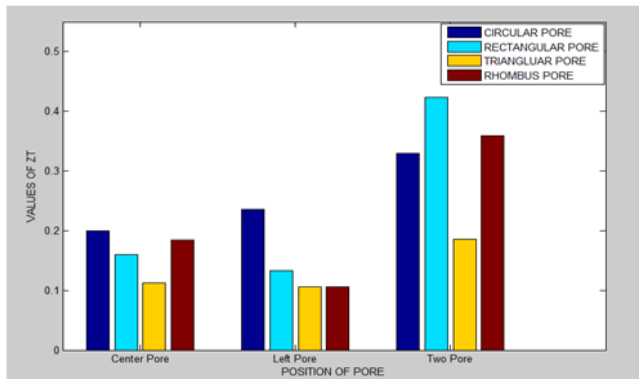


Fig. 10 Comparison of the figure of merit for all the pore shapes and pore positions

To investigate the shape dependent and position dependent thermoelectric properties, we compare the results obtained for all the pore shapes and their respective positions. The value of maximum ZT is extracted for different cases Fig (10) shows the comparison between the various values of ZT obtained. It is analyzed that in case of single pore nanoribbon, the figure of merit of individual pore shape is not affected much by variation of pore position. Moreover the circular shape pore shows the maximum figure of merit followed by rectangular pore and triangular pore being the least. Further, triangular pore shows similar results with change in pore position from centre to left. The order of thermoelectric performance is CIRCULAR>RECTANGULAR>RHOMBUS>TRIANGULAR.

In case of double pore the optimum performance is shown by rectangular pore. The order of figure of merit is RECTANGULAR>RHOMBUS>CIRCULAR>TRIANGULAR. The increase in ZT with multiple pores is increased significantly in rectangular pore as compared to other pore shapes. Overall, the rectangular shaped pores are most favorable to obtain thermoelectric performance in GNR.

V. PORE PASSIVATION

In addition, the influence of passivation of the pore edges on the thermoelectric performance of GNRs has been analyzed. The porous results obtained for passivated pore edges for all the four shapes are then compared with the non passivated results obtained so far as demonstrated in Fig 11(a-d). As observed for Fig 12(c), the effects of pore passivation are not much pronounced for the circular shapes since there is a very little or no effect on the thermoelectric performance with pore passivation. However, overall improvement has been observed for triangular pores as shown in Fig 12(d) with an enhancement in G and ZT. Although, The pore passivation results in a dramatic improvement in G for rectangular pore and S for rhombus pore, but the corresponding decrease in the other thermoelectric performance parameters compensates for the increase resulting in no improvement in overall thermoelectric figure of merit.

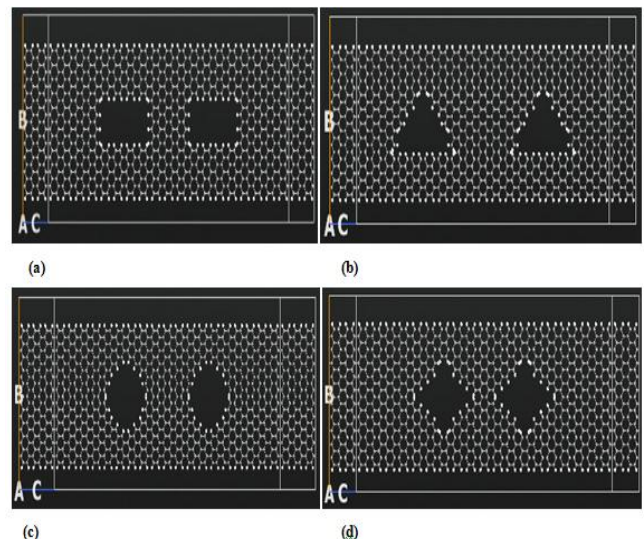


Fig. 11 passivated double pores (a) rectangular pore, (b) triangular pore, (c) circular pore, and (d) rhombus pore

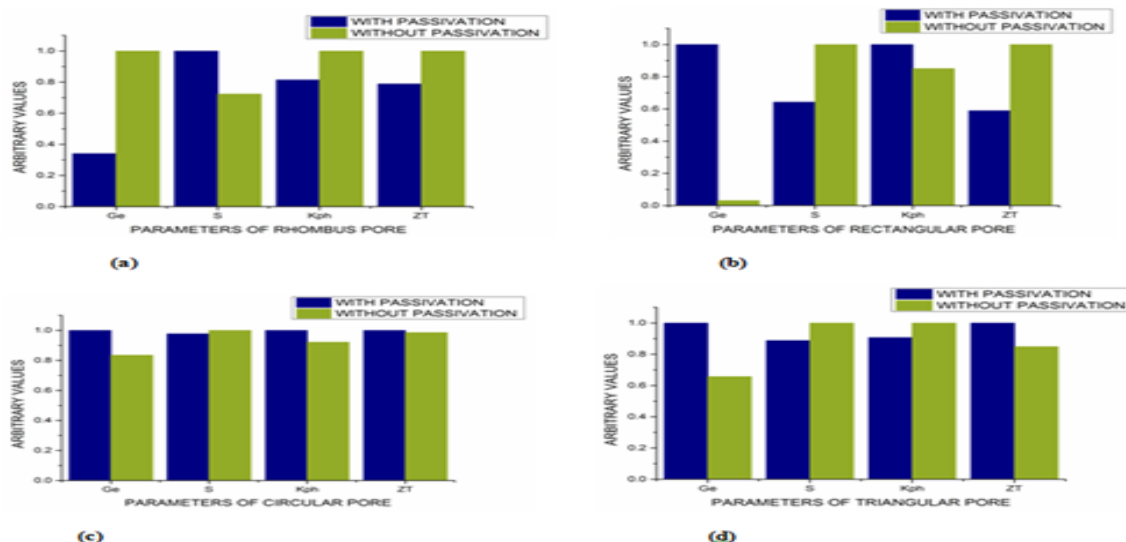


Fig. 12 Comparison of the various parameters of the passivated and nonpassivated pores for (a) rhombus pore, (b) rectangular pore, (c) circular pore, and (d) triangular pore

VI. TEMPERATURE DEPENDENCE

Fig (13) illustrates the effects of temperature dependence on the thermoelectric performance of single porous nanostructure (rectangular in this case). It is seen that the temperature affects the figure of merit greatly. The power factor (S^2G) decreases linearly and then it becomes stable from 650K. The K_e and K_{ph} increases simultaneously. The sum of K_e and K_{ph} equates to the K which denotes the

thermal conductivity. At low temperatures of 150K higher values of figure of merit is observed. But a sudden decrease in value of ZT is noticed for intermediate temperature extending till 500K. However, for higher temperatures, the value of ZT increases linearly and reaches at highest value at nearly 1100K. We need low thermal conductivity and higher power factor to achieve higher figure of merit. To achieve a better figure of merit delicate optimization of these factors should be done as these factors are correlated.

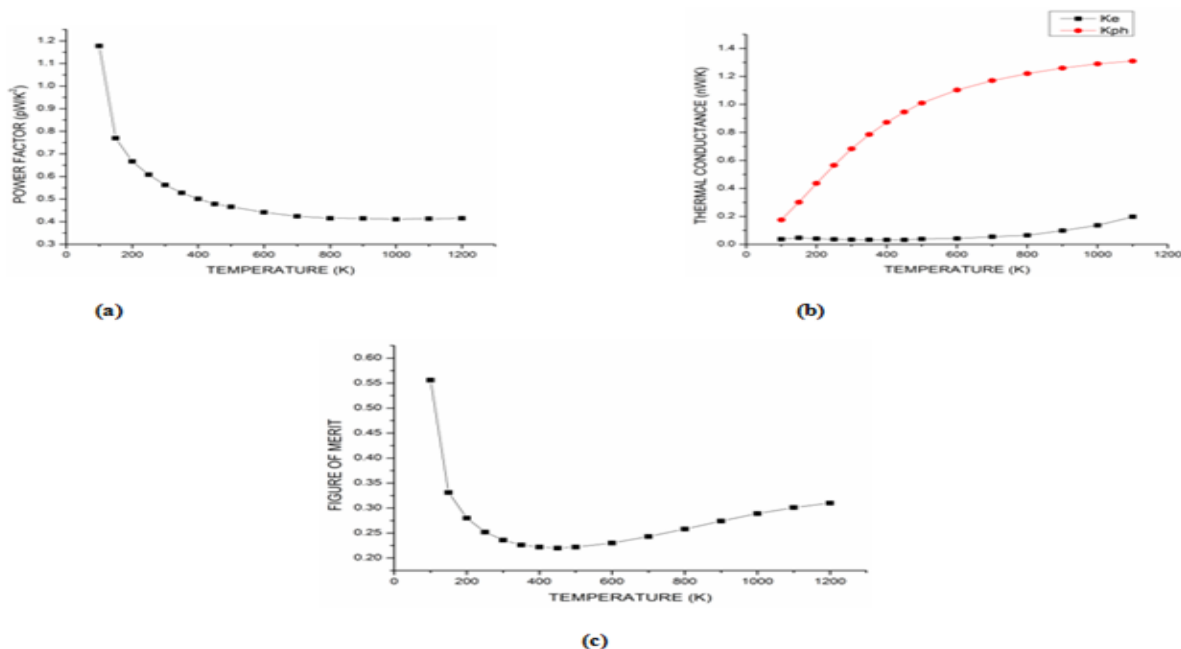


Fig. 13 Temperature dependence of the (a) thermal conductance, (b) figure of merit, (c) power factor for the rectangular single pore GNR structure

VII. CONCLUSION

In summary, we have investigated the effect of pore shapes and their positions on the thermoelectric performance of GNRs nanoporous devices. Nanopores of different shapes

i.e. circular, rectangular, triangular and rhombus have been introduced at varying positions of the nano structure so as to study their effect on the thermoelectric figure of merit. By optimizing the pore parameters, we have been able to achieve higher thermoelectric figure of merit which is four

times higher than GNR without any pore. Further, the effect of pore passivation is observed which has been successfully able to enhance ZT in case of triangular pores. Thus, our work extends the idea towards achieving better thermoelectric devices by optimal pore engineering.

REFERENCES

- [1] M.S. Hossain, F. Al-Dirini, F.M. Hossain, and E. Skafidas, "High performance graphenenano-ribbon thermoelectric devices by incorporation and dimensional tuning of nanopores". *Sci. Rep.* Vol. 5, 11297, June 2015.
- [2] L.D. Hicks and M.S. Dresselhaus, "Thermoelectric figure of merit of a one-dimensional conductor". *Phys. Rev. B*, Vol. 47, pp. 16631–16634, June 1993.
- [3] N. Mingo and D.A. Broido, "Thermoelectric power factor of nanoporous semiconductors". *J. Appl. Phys.* Vol. 101, 014322, Jan. 2007.
- [4] H. Sadeghi, S. Sangtarash, and C.J. Lambert, "Enhanced thermoelectric efficiency of porous silicone nanoribbons", *Sci. Rep.* Vol. 5, 9514, Mar 2015.
- [5] M.S. Hossain, F. Al-Dirini, F.M. Hossain, and E. Skafidas, "High performance graphene nano-ribbon thermoelectric devices by incorporation and dimensional tuning of nanopores", *Sci. Rep.* Vol. 5, 11297, June 2015.
- [6] Y. Ouyang, and J. Guo, "A theoretical study on thermoelectric properties of graphene nanoribbons", *Appl. Phys. Lett.* Vol. 94, 263107, June 2009.
- [7] Y. Xu, Z. Li, and W. Duan, "Thermal and thermoelectric properties of graphene", *Nano Micro Small*, Vol. 10, pp. 2182-2199, June 2014.
- [8] C.N. Pan, Z.X. Xie, L.M. Tang, and K.Q. Chen, "Ballistic thermoelectric properties in graphene-nanoribbon-based heterojunctions", *Appl. Phys. Lett.* Vol. 101, 103115, Sept. 2012.
- [9] L.B. Liang, E. Cruz-Silva, E.C. Girao, and V. Meunier, "Enhanced thermoelectric figure of merit in assembled graphene nanoribbons", *Phys. Rev. B: Condens. Matter Mater. Phys.* Vol. 86, 115438, Sept. 2012.
- [10] H. Sevincli and G. Cuniberti, "Enhanced thermoelectric figure of merit in edge-disordered zigzag graphene nanoribbons", *Phys. Rev. B: Condens. Matter Mater. Phys.* Vol. 81, pp. 113401–113404, March 2010.
- [11] J.G. Checkelsky and N.P. Ong, "Thermopower and Nernst effect in graphene in a magnetic field", *Phys. Rev. B: Condens. Matter Mater. Phys.* Vol. 80, 081413, Aug 2009.
- [12] D. Wang and J. Shi, "Effect of charged impurities on the thermoelectric power of graphene near the Dirac point", *Phys. Rev. B: Condens. Matter Mater. Phys.* Vol. 83, 113403, March 2011.
- [13] P. Wei, W. Bao, Y. Pu, C.N. Lau, and J. Shi, "Anomalous thermoelectric transport of Dirac particles in graphene", *Phys. Rev. Lett.* Vol. 102, 166808, April 2009.
- [14] F. Mazzamuto, V.H. Nguyen, Y. Apertet, C. Caer, C. Chassat, J. Saint-Martin, and P. Dollfus, "Enhanced thermoelectric properties in graphenenanoribbons by resonant tunneling of electrons", *Phys. Rev. B: Condens. Matter Mater. Phys.* Vol. 83, 235426, June 2011.
- [15] L.B. Liang, E. Cruz-Silva, E.C. Girao, and V. Meunier, "Enhanced thermoelectric figure of merit in assembled graphene nanoribbons", *Phys. Rev. B: Condens. Matter Mater. Phys.* Vol. 86, 115438, Sept. 2012.
- [16] F. Mazzamuto, J. S. Martin, V.H. Nguyen, C. Chassat, and P. Dollfus, "Thermoelectric performance of disordered and nanostructured graphene ribbons using Green's function method". *J. Comput. Electron.* Vol. 11, pp. 67–77, March 2012.
- [17] M.Y. Han, B. Ozyilmaz, Y.B. Zhang, and P. Kim, "Energy bandgap engineering of graphene nanoribbons", *Phys. Rev. Lett.* Vol. 98, 206805, May 2007.
- [18] J. Bai, X. Duan, and Y. Huang, "Rational fabrication of graphene nanoribbons using a nanowire etch mask", *Nano Lett.* Vol. 9, pp. 2083–2087, April 2009.
- [19] Z. Wei, Z. Qiang, Z. Meng-Qiang, and L.T. Kuhn, "Direct writing on graphene 'paper' by manipulating electrons as 'invisible ink'", *Nanotechnology*, Vol. 24, pp. 1–6, June 2013.
- [20] L. Tapasztó, G. Dobrik, P. Lambin, and L.P. Biro, "Tailoring the atomic structure of graphene nanoribbons by scanning tunnelling microscope lithography", *Nat. Nanotechnol.* Vol. 3, pp. 397–401, June 2008.
- [21] N. Kalthor, S.A. Boden, and H. Mizuta, "Sub-10 nm patterning by focused He-ion beam milling for fabrication of downscaled graphene nano devices", *Microelectron. Eng.* Vol. 114, pp. 70–77, Feb. 2014.
- [22] A.N. Abbas, G. Liu, B. Liu, L. Zhang, H. Liu, D. Ohlberg, W. Wu, and C. Zhou, "Patterning, characterization, and chemical sensing applications of graphene nanoribbon arrays down to 5 nm using helium ion beam lithography", *ACS Nano*, Vol. 8, pp. 1538–1546, Jan. 2014.
- [23] D. Kienle, J.I. Cerda, and A.W. Ghosh, "Extended Huckel theory for band structure, chemistry, and transport. I. Carbon nanotubes", *J. Appl. Phys.* Vol. 100, 043714, Aug 2006.
- [24] K. Esfarjani, M. Zebarjadi, and Y. Kawazoe, "Thermoelectric properties of a nanocontact made of two-capped single-wall carbon nanotubes calculated within the tight-binding approximation", *Phys. Rev. B: Condens. Matter Mater. Phys.* Vol. 73, 085406, Feb. 2006.
- [25] H. Sadeghi, S. Sangtarash, and C.J. Lambert, "Enhancing the thermoelectric figure of merit in engineered graphene nanoribbons", *Beilstein J. Nanotechnol.* Vol. 6, pp. 1176–1182, March 2015.
- [26] R. Landauer, "Spatial variation of currents and fields due to localized scatterers in metallic conduction", *IBM. J. Res. Dev.* Vol. 1, pp. 223–231, July 1957.
- [27] K. Stokbro, D.E. Peterson, S. Smidstrup, A. Blom, M. Ipsen, and K. Kaasbjerg, "Semi empirical model for nanoscale device simulations", *Phys. Rev. B: Condens. Matter Mater. Phys.* Vol. 82, 075420, August 2010.
- [28] J.H. Chen, C. Jang, S. Xiao, M. Ishigami, and M.S. Fuhrer, "Intrinsic and extrinsic performance limits of graphene devices on SiO₂", *Nat. Nano.* Vol. 3, pp. 206–209, April 2008.
- [29] S. Kaur, S. B. Narang, D. K. Randhawa, "Influence of the pore shape and dimension on the enhancement of thermoelectric performance of graphene nanoribbons", *Sci. Rep.* Vol. 32, pp. 1-11, Dec.2016